Joint Average Spectrum-Texture Representation in Hyperspectral Images using Relocated Spectral Difference Occurrence Matrix

Rui Jian CHU[1], Noël RICHARD[1], Christine FERNANDEZ-MALOIGNE[1], Jon Yngve HARDEBERG[2]

[1]Université de Poitiers, CNRS, XLIM, UMR 7252, F-86000 Poitiers, France

[2]Department of Computer Science, Norwegian University of Science and Technology, Norway

rui.jian.chu01@univ-poitiers.fr, noel.richard@univ-poitiers.fr,
christine.fernandez@univ-poitiers.fr, jon.hardeberg@ntnu.no

Résumé – Pour l'analyse métrologique des images hyperspectrales, nous proposons un attribut texture associant spectre moyen et différences spectrales, appelé *Relocated Spectral Difference Occurrence matrix* (rSDOM). Cet attribut extrait les différences entre pixels voisins pour produire un attribut dense et générique quel que soient les plages et résolution spectrales. Le rSDOM est validé dans un schéma de classification utilisant la base HyTexiLa et obtient une précision comparable à celle de l'état de l'art pour une taille d'attribut extrêmement réduite.

Abstract – In the metrological framework of hyperspectral image processing, we propose a texture feature named *Relocated Spectral Difference Occurrence matrix* (rSDOM). It processes the spectral differences between neighbouring pixels to produce a dense and generic feature independent from the spectral range and resolutions. It has been validated in a classification scheme using HyTexiLa dataset, producing comparable accuracy to Opponent Band Local Binary Pattern (OBLBP) but with an extremely small feature size.

1 Introduction

Texture or non-uniformity assessment has become one of the main disciplines in image processing since the introduction of co-occurrence matrix by Haralick in 1973 [1]. Since then, there has been countless work in the gray-scale domain [2, 3, 4]. The extension to color or spectral domains, however, is not so straightforward as the color or spectral channels are often correlated, prohibiting marginal processing. Besides, hyperspectral image processing often suffers from the curse of dimensionality. The numerous number of channels, sometimes up to hundreds contain redundant information and make computation extremely complex. To solve this issue, the common strategy is to perform band selection [5] or dimensionality reduction [6] using principal component analysis (PCA), non-negative matrix factorization (NMF), and others.

However, the metrological aspect of such approach is rarely studied. Following the sampling operation, an acquired spectrum using a hyperspectral sensor is represented as a discrete sequence of measurements $S = [s(\lambda_1), s(\lambda_2), ..., s(\lambda_L)]$ for L spectral bands. Due to its discrete representation, an acquired spectrum is often considered as a set of independent measures and hence associated with L2-norm for spectral difference assessment. Such definition neglects the importance of order in the acquired spectra values and its limits has been elaborated in the work of [7]. Consequently, Kullback-Leibler pseudo-divergence (KLPD) is proposed [8] to assess spectral difference in accordance to the metrological constraints, of which the feature described in this work is based on.

According to the first Julesz conjecture, preattentive discrimination of textures is possible only for textures that differ on second-order statistics [9]. Following this definition, we take inspiration from the pioneering work of Haralick [1] and Ojala [4], namaly the co-occurrence matrix and Local Binary Pattern (LBP). The texture description using co-occurrence matrix is complete, but its reduction into moments for similarity measure causes information losses. For LBP, the binarization provides a weak characterization of texture, but its similarity measure is extremely efficient. Following the work of [10] which relates co-occurrence matrix and histogram of differences, we combine the strength of both approaches and adapt it in the domain of hyperspectral image processing while respecting the metrological constraints. For enhanced efficiency, we decide to incorporate average spectrum in the texture feature, thus inducing a joint average-spectrum-texture formulation.

The rest of the article is organized in the following manner. Section 2 describes the mathematical formulation of the feature. Next, Section 3 presents the evaluation of the feature. Finally, Section 4 lists the concluding remarks for this work.

2 Joint average spectrum-texture feature

We begin by first recalling the formulation of spectral difference based on KLPD [8]. Next, we propose a texture feature and proceed to model it for compact representation. Then, we develop the similarity measure and finally present the final form of the joint average spectrum-texture feature.

2.1 Assessing spectral difference

The formulation of KLPD [8] is inspired from Kullback-Leibler (KL) divergence between two normalized spectra (eq. 5). Designed to be symmetrical, the spectral difference between two spectra S_1 and S_2 is expressed as :

$$d_{KLPD}(S_1, S_2) = \Delta G(S_1, S_2) + \Delta W(S_1, S_2) \quad (1)$$

which consists of spectral shape difference ΔG, given by :

$$\Delta G(S_1, S_2) = k_1 \cdot KL(\bar{S}_1 \| \bar{S}_2) + k_2 \cdot KL(\bar{S}_2 \| \bar{S}_1) \quad (2)$$

and spectral intensity difference ΔW, given by :

$$\Delta W(S_1, S_2) = (k_1 - k_2) \log\left(\frac{k_1}{k_2}\right) \quad (3)$$

where :

$$KL(\bar{S}_1 \| \bar{S}_2) = \int_{\lambda_{\min}}^{\lambda_{\max}} \bar{S}_1(\lambda) \cdot \log \frac{\bar{S}_1(\lambda)}{\bar{S}_2(\lambda)}\, d\lambda \quad (4)$$

$$\bar{S}_j = \left\{ \bar{s}_j(\lambda) = \frac{s_j(\lambda)}{k_j},\ \forall \lambda \in [\lambda_{\min}, \lambda_{\max}] \right\}, j \in \{1, 2\}$$
$$\text{and } k_j = \int_{\lambda_{\min}}^{\lambda_{\max}} s_j(\lambda)\, d\lambda, j \in \{1, 2\} \quad (5)$$

2.2 Spectral Difference Occurrence matrix

For a hyperspectral image $H \in \mathbb{R}^{N \times L}$ with N pixels and L spectral bands, the Spectral Difference Occurrence matrix (SDOM) M is a probability density function given by :

$$M^{(d,\theta)}(\Delta G, \Delta W) = Prob\Big(d_{KLPD}(S_i, S_j) = (\Delta G, \Delta W) \Big), \quad \forall i, j \in H, \|\overrightarrow{ij}\| = l, \angle\overrightarrow{ij} = \theta \quad (6)$$

where S_i and S_j are the i^{th} and j^{th} pixels separated by distance l in the direction θ, while ΔG and ΔW are spectral shape and intensity differences as defined in eq. 2 and eq. 3 respectively.

For representation in compact form, we proceed to apply statistical modelling on SDOM. For textured images, there are four possible pixel pairs : (a) (background, background), (b) (texton, texton), (c) (background, texton) and (d) (texton, background). Their spectral differences is thus multimodal, with one group (of smaller values) belonging to (a) and (b), and the other (of larger values) belonging to (c) and (d). Due to noise and sensor resolution limits, one can expect the spectral differences to be approximately normally distributed. This necessitates the use of Gaussian mixture model (GMM), which models SDOM using a mixture of K Gaussian distributions $\mathcal{N}$:

$$M = \sum_{i=1}^{K} \phi_i \mathcal{N}(\mu_i, \Sigma_i) \quad (7)$$

where ϕ is the mixture weight. Thus using GMM, SDOM can be modelled using just $K \times (1 + D + D^2)$ scalar values, where D is the number of dimension (for SDOM, $D = 2$). In this work, we choose+ to select $K = 3$ though in future, a set of protocols for selecting the optimum K is to be developed.

2.3 Similarity measure using Kullback-Leibler divergence

To discriminate between texture, a similarity measure between SDOM is to be developed. As SDOM is a probability density function, KL divergence [11] has been identified as the most efficient similarity measure [12]. For two multivariate Gaussian distributions $f \sim \mathcal{N}(\mu_1, \Sigma_1)$ and $g \sim \mathcal{N}(\mu_2, \Sigma_2)$, the KL divergence from f to g has a closed form solution [13] :

$$KL(f\|g) = \frac{1}{2}\Bigg[\log\frac{|\Sigma_2|}{|\Sigma_1|} + \mathrm{tr}(\Sigma_2^{-1}\Sigma_1) - D + (\mu_2 - \mu_1)^T \Sigma_2^{-1} (\mu_2 - \mu_1) \Bigg] \quad (8)$$

where D is the dimension of the data. However, there exists no closed form solution for KL divergence between two GMMs. By variational approximation [14], the KL divergence of two SDOM from M to M' is approximated as :

$$KL(M\|M') \overset{\text{var}}{\approx} \sum_i \phi_i \log \frac{\sum_{i'} \phi_{i'} e^{-KL(M_i\|M_{i'})}}{\sum_j \phi'_j e^{-KL(M_i\|M'_j)}} \quad (9)$$

as $M = \sum_i \phi_i M_i$ and $M' = \sum_j \phi'_j M'_j$. As KL divergence is not symmetric, that is, $KL(M\|M') \neq KL(M'\|M)$, the similarity measure is given by :

$$d_{KL}(M, M') = KL(M\|M') + KL(M'\|M) \quad (10)$$

2.4 Joint average spectrum-texture feature

SDOM assesses only the local spatial variation and by construction, is invariant to spectral information of the image. To increase texture discrimination, we modify SDOM into Relocated Spectral Difference Occurrence Matrix (rSDOM), $\hat{M}$:

$$\hat{M} = \{S_{avg}, M\} \quad (11)$$

where S_{avg} is the average spectrum defined marginally as :

$$S_{avg} = \left\{ s_{avg}(\lambda) = \frac{1}{N} \sum_{i=1}^{N} s(\lambda), \forall \lambda \in [\lambda_{\min}, \lambda_{\max}] \right\} \quad (12)$$

where N is the number of pixels in the hyperspectral image. The similarity measure of rSDOM is given by :

$$d_{KL}(\hat{M}, \hat{M'}) = d_{KL}(M + \Delta_S, M') \quad (13)$$

where Δ_S is the spectral difference between the two average spectra using KLPD. Note that rSDOM has a feature size of $K \times (1 + D + D^2) + L$, where L is the spectral count.

3 Experiment and discussion

We introduce the hyperspectral dataset and describe the protocols of evaluation. Then, we analyze the result and discuss the performance of rSDOM. Finally, we list the limitations of rSDOM and propose some future work.

3.1 Classification using nearest neighbor

To assess the efficiency of rSDOM, we apply a classification scheme on HyTexiLa [15]. The dataset consists of 112 hyperspectral images with $N = 1024 \times 1024$ and $L = 186$, categorized into *Food* (10 images), *Stone* (4), *Textile* (65), *Wood* (18) and *Vegetation* (15). The spectral range is from 405 nm to 995 nm, thus spanning the visible and near infrared region.

For classification, each image is divided into 25 patches with $N = 204 \times 204$, among which 12 is randomly selected for training and 13 for testing. For simplicity, we perform the classification using 1-nearest neighbor approach. We perform both inter-categorical classification (denoted as *All* in Table 1) and intra-categorical classification. To demonstrate the superiority of joint average spectrum-texture representation by rSDOM, we present three classification results based on average spectrum (avg. spe.), SDOM and rSDOM. We repeat each classification 10 times and present the average classification accuracy with standard error. In this work, we choose $l = 3$ and $\theta = 0$.

3.2 Result and analysis

Figure 1 illustrates SDOM for "coffee" and "milkcoffee" (rendered in sRGB) from HyTexiLa. In terms of spectral shape difference, both SDOM are about the same because both are of the same substance albeit at different processing level. In terms of spectral intensity difference, the SDOM of "coffee" is more varied than "milkcoffee" due to the difference in granular size and hence the light interaction. This shows that SDOM (and rSDOM) is able to discriminate texture in a clear representation.

From Table 1, the performance of rSDOM is excellent with an accuracy of 95.9 % and precision / recall of 96.2 % / 95.9 % (in inter-categorical classification). We also note that the classification using rSDOM (85.0 % - 100.0 %) outperforms both average spectrum (78.2 % - 98.6 %) and SDOM (63.0 % - 91.2 %). This demonstrates the added advantage of incorporating average spectrum in hyperspectral texture recognition.

To explain the misclassification, we first note our choice of $l = 3$ limits us from assessing texture with large texton size. This explains our better classification for *Food*, *Stone* and *Textile* images which consist of mainly fine textons, but lower score for *Wood* and *Vegetation* images with larger texton size. Moreover, our unitary choice of θ allows us to only evaluate texture in one direction. In fact, for $\theta = 0$ we are only able to assess texture varying in vertical direction but not in other directions. This is acceptable for isotropic texture, but not adapted for anisotropic one such as those found in *Vegetation* and *Wood*.

In comparison to [15] which reports an maximum accuracy of 98.76 % using Opponent Band Local Binary Pattern (OBLBP) with 18 equally spaced spectral bands, our performance is lower (95.9 %) although in the same efficiency range. The difference in performance can be attributed to the fact that OBLBP assesses texture in eight directions while rSDOM evaluates just one. However, it is worthwhile to mention that the feature size of rSDOM is extremely small. For 18 spectral bands and texture assessment in 8 directions, OBLBP consists of 82944 scalar values. By contrast, the size of rSDOM is only $K \times (1 + D + D^2) + L = 21 + 186 = 207$ scalar values or 0.25 % of OBLBP's. This presents rSDOM as an extremely compact texture descriptor for rapid processing and storage.

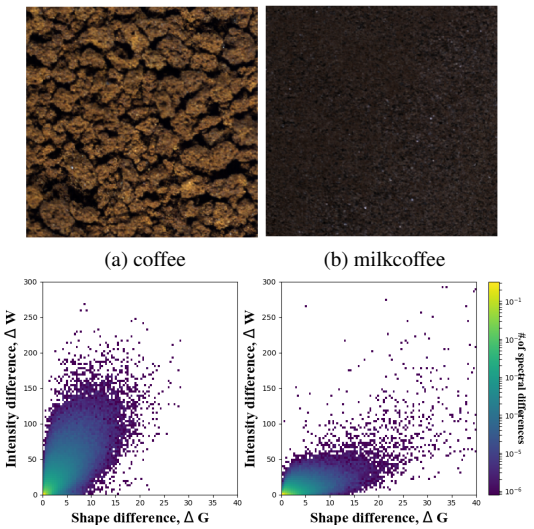

FIGURE 1 – SDOM of "coffee" and "milkcoffee".

3.3 Limitations and future work

The choice of $l = 3$ remain questionable, as it is possibly susceptible to image noise and it is expected that a larger l value could present better result. In fact, as texture varies in scale and direction, rSDOM could benefit from a multi-scale and multi-direction implementation. On the other hand, the choice of using variational approximation in this work to evaluate divergence between two rSDOM which are GMMs remains to be justified. Other methods ought to be studied in order to deter-

TABLE 1 – Classification accuracy on HyTexiLa database.

Category	Avg. spe. (%)	SDOM (%)	rSDOM (%)
All	91.9 ± 0.2	72.2 ± 0.3	$\mathbf{95.9 \pm 0.2}$
Food	95.1 ± 0.3	91.2 ± 0.6	$\mathbf{97.3 \pm 0.3}$
Stone	84.6 ± 1.5	88.5 ± 0.9	$\mathbf{100.0 \pm 0.0}$
Vegetation	82.9 ± 0.9	63.0 ± 0.7	$\mathbf{89.4 \pm 0.7}$
Wood	78.2 ± 0.9	63.5 ± 1.0	$\mathbf{85.0 \pm 0.8}$
Textile	98.6 ± 0.1	78.4 ± 0.4	$\mathbf{98.9 \pm 0.1}$

mine the best distance measure. Besides, it has to be clarified that the choice of $K = 3$ or using three GMMs to model rSDOM in this work is arbitrary. The optimum K value remains to be identified or perhaps, K could be designed to vary depending on the texture.

4 Conclusion

We have proposed a joint average spectrum-texture feature, rSDOM for hyperspectral images which is compact and computationally simple. It describes the local spectral differences and takes into account the average spectrum of the image. The proposed feature is in full accordance with the psychophysical experiments on texture while respecting the metrological constraints. It is generic and is adapted for any number of spectral band and range. Its performance has been evaluated via classification on HyTexiLa with excellent results, considering the fact that the feature is only evaluated on single scale ($l = 3$) and direction ($\theta = 0$). The classification accuracy is comparable to Opponent Band Local Binary Pattern (OBLBP), but at a much smaller feature size (0.25 % of OBLBP). This proves interesting for applications such as remote sensing whereby feature size is essential for transmission purposes.

Références

[1] R.M. Haralick, K. Shanmugam, and I. Dinstein. "Textural feature for image classification," in *IEEE Trans. on System Man and Cybernetics*. vol. 3(6), pp. 610–621, 1973.

[2] Mary M. Galloway. "Texture analysis using gray level run lengths," in *Computer Graphics and Image Processing*. vol. 4(2), pp. 172–179, 1975.

[3] Jing Huang, S. R. Kumar, M. Mitra, Wei-Jing Zhu, and R. Zabih. "Image indexing using color correlograms," in *Proc. of IEEE Computer Society Conference on Computer Vision and Pattern Recognition*. pp. 762–768, 1997.

[4] Timo Ojala, Matti Pietikainen and Topi Maenpaa. "Multiresolution gray-scale and rotation invariant texture classification with L. B. P.," in *IEEE Trans. on Pattern Anal. and Machine Intel.*. vol. 24(7), pp. 971–987, 2002.

[5] S. Le Moan, A. Mansouri, Y. Voisin and J. Y. Hardeberg, "A constrained band selection method based on information measures for spectral image color visualization", in *IEEE Transactions on Geoscience and Remote Sensing*. vol. 49 (12), pp. 5104-5115, 2011.

[6] H. Zeng and H. J. Trussell. "Dimensionality reduction in hyperspectral image classification," in *2004 International Conference on Image Processing, 2004. ICIP '04*. vol. 2, pp. 913-916, 2004.

[7] H. Deborah, N. Richard, J. Y. Hardeberg, and C. Fernandez-Maloigne. "Assessment protocols and comparison of ordering relations for spectral image processing," in *IEEE Journal of Selected Topics in Applied Earth Observations and Remote Sensing*. vol. 11(4), pp. 1253–1265, 2018.

[8] N. Richard, D. Helbert, C. Olivier, and M. Tamisier. "Pseudo-divergence and bidimensional histogram of spectral differences for hyperspectral image processing," in *J. Imaging Sci. Techn.*. vol. 60(5), pp. 1–13, 2016.

[9] B. Julesz. "Visual pattern discrimination," in *Transactions on Information Theory*. vol. 8(2), pp. 84–92, 1962.

[10] M Unser. "Sum and difference histograms for texture classification," in *IEEE Trans. on Pattern Anal. and Machine Intel.*. vol. 8(1), pp. 118–125, 1986.

[11] S. Kullback and R. A. Leibler, "On information and sufficiency," in *The Annals of Mathematical Statistics*. vol. 22(1), pp. 79–86, 1951.

[12] Z. Bylinskii, T. Judd, A. Oliva, A. Torralba, and F. Durand. "What do different evaluation metrics tell us about saliency models ?" in *IEEE Trans. on Pattern Anal. and Machine Intel.*. vol. 41(3), pp. 740-757, 2019.

[13] CE. Rasmussen and CKI. Williams. *Gaussian Processes for Machine Learning*. MIT Press, 2006.

[14] John R. Hershey and Peder A. Olsen. "Approximating the Kullback Leibler Divergence Between Gaussian Mixture Models," in *2007 IEEE International Conference on Acoustics, Speech and Signal Processing - ICASSP '07*. pp. IV-317-IV-320, 2007.

[15] Haris Ahmad Khan, Sofiane Mihoubi, Benjamin Mathon, Jean-Baptiste Thomas, and Jon Yngve Hardeberg "Hytexila : High resolution visible and near infrared hyperspectral texture images," in *Sensors*. vol. 18(7), 2018.